Release of ATP and glutamate in the nucleus tractus solitarii mediate pulmonary stretch receptor (Breuer–Hering) reflex pathway

Alexander V. Gourine[1], Nicholas Dale[2], Alla Korsak[1], Enrique Llaudet[2], Faming Tian[2], Robert Huckstepp[2] and K. Michael Spyer[1]

[1] *Department of Physiology, University College London, Gower Street, London WC1E 6BT, UK*
[2] *Department of Biological Sciences, University of Warwick, Coventry CV4 7AL, UK*

The Breuer–Hering inflation reflex is initiated by activation of the slowly adapting pulmonary stretch receptor afferents (SARs), which monosynaptically activate second-order relay neurones in the dorsal medullary nucleus of the solitary tract (NTS). Here we demonstrate that during lung inflation SARs release both ATP and glutamate from their central terminals to activate these NTS neurones. In anaesthetized and artificially ventilated rats, ATP- and glutamate-selective microelectrode biosensors placed in the NTS detected rhythmic release of both transmitters phase-locked to lung inflation. This release of ATP and glutamate was independent of the centrally generated respiratory rhythm and could be reversibly abolished during the blockade of the afferent transmission in the vagus nerve by topical application of local anaesthetic. Microionophoretic application of ATP increased the activity of all tested NTS second-order relay neurones which receive monosynaptic inputs from the SARs. Unilateral microinjection of ATP into the NTS site where pulmonary stretch receptor afferents terminate produced central apnoea, mimicking the effect of lung inflation. Application of P2 and glutamate receptor antagonists (pyridoxal-5′-phosphate-6-azophenyl-2′,4′-disulphonic acid, suramin and kynurenic acid) significantly decreased baseline lung inflation-induced firing of the second-order relay neurones. These data demonstrate that ATP and glutamate are released in the NTS from the central terminals of the lung stretch receptor afferents, activate the second-order relay neurones and hence mediate the key respiratory reflex – the Breuer–Hering inflation reflex.

(Received 27 March 2008; accepted after revision 26 June 2008; first published online 10 July 2008)
Corresponding author A. V. Gourine: Department of Physiology, University College London, Gower Street, London WC1E 6BT, UK. Email: a.gourine@ucl.ac.uk

The central respiratory network located in the medulla oblongata and pons is responsible for generation of the respiratory rhythm. The network also includes premotor neurones which transmit this rhythm to spinal motorneurones controlling the diaphragm and intercostal muscles (Feldman *et al.* 2003; Feldman & Del Negro, 2006). The major afferent inputs to the brainstem respiratory network that influence its activity originate from the central and peripheral arterial chemoreceptors and from the pulmonary stretch receptors that provide information about the mechanical status of the lungs and the chest. Activation of slowly adapting pulmonary stretch receptors (SARs) during lung inflation initiates the Breuer–Hering reflex – a key negative feedback mechano-reflex controlling the duration of inspiration (Breuer, 1868; Head, 1889; Adrian, 1933; Widdicombe, 2001). SARs monosynaptically transmit information about lung volume to the second order relay neurones or pump cells located in a discrete region of the dorsal medullary nucleus of the solitary tract (NTS) at the level of the area postrema and adjacent to the tractus solitarius (Bonham & McCrimmon, 1990; Miyazaki *et al.* 1999; Kubin *et al.* 2006). Pump cells relay the information obtained from SARs to the medullary and pontine respiratory networks (Ezure *et al.* 2002; Kubin *et al.* 2006) to evoke rapid suppression of inspiratory activity. Several studies have demonstrated that activation of the pump cells by the SARs input is at least partly mediated by the action of glutamate at excitatory amino acid (EAA) receptors (most likely of AMPA type) (Bonham *et al.* 1993; Zhang & Mifflin, 1995; Miyazaki *et al.* 1999; Kubin *et al.* 2006).

 DOI: 10.1113/jphysiol.2008.154567

Specific ATP receptors, both ionotropic P2X and metabotropic P2Y, are widely expressed in the CNS by both neurones and glia. Although there are few central synapses where fast neurotransmission is predominantly mediated via release of ATP and activation of post-synaptic P2X receptors (Edwards *et al.* 1992; Khakh & North, 2006; Burnstock, 2007), ATP can be released as a cotransmitter (Jo & Schlichter, 1999; see Pankratov *et al.* 2006 for review). In the cortex (Pankratov *et al.* 2002, 2003) and hippocampus (Pankratov *et al.* 1998), glutamatergic EPSCs contain a small P2X receptor-mediated component that is mediated through quantal release of ATP (Pankratov *et al.* 2007).

ATP receptors are distributed widely throughout the brainstem and in the NTS the density of neurones and nerve fibres that contain ionotropic P2X receptors is remarkably high (Kanjhan *et al.* 1999; Yao *et al.* 2000, 2001, 2003). Given the abundance of ATP receptors in the NTS and the precedent of cotransmssion by ATP and glutamate, we examined the contribution of ATP signalling to transmission at the central synapses of the SARs. First, ATP- and glutamate-selective biosensors were used to determine whether ATP and glutamate are released in the NTS during lung inflation. Then, the effect of exogenous ATP on breathing and discharge patterns of different types of NTS neurones was determined. Finally, the effects of P2 and EAA receptor antagonists applied individually or simultaneously on the activity of the NTS pump cells were examined.

Methods

Surgical procedures

Experiments were performed on 43 male Sprague–Dawley rats (300–340 g) and carried out in accordance with the UK Animals (Scientific Procedures) Act, 1986. The rats were anaesthetized with pentobarbitone sodium (60 mg kg^{-1}, I.P.). Anaesthesia was maintained with supplemental doses of pentobarbitone sodium injected intravenously as required (10 mg kg^{-1} h^{-1}). Adequate anaesthesia was ensured by maintaining stable levels of arterial blood pressure (ABP), heart and central respiratory rate. The femoral artery and vein were cannulated for measurement of ABP and administration of anaesthetic, respectively. The trachea was cannulated and the animal was ventilated with O_2-enriched air using a positive pressure ventilator with a tidal volume of 1.5–2.0 ml and a ventilator frequency similar to the normal respiratory frequency ($\sim$60 strokes min^{-1}). The animal was then injected with gallamine triethiodide (Flaxedil, 10 mg kg^{-1}, I.V.; then 1–2 mg kg^{-1} h^{-1}, I.V.) and was placed in a stereotaxic frame. An occipital craniotomy was performed and the cerebellum was partially removed to expose the dorsal surface of the brainstem. The exposed area of the brain was protected by covering with modified Bulmer's buffer, which consisted of (mM): 100 NaCl, 1 $MgSO_4$, 2 KPi buffer, 5 glycerol (pH 7.4).

Activity of the phrenic nerve was recorded as an indicator of central respiratory drive. The signal was amplified ($\times$20 000), filtered (500–1500 Hz), rectified and smoothed ($\tau = 100$ ms). The vagus nerve was isolated from the surrounding tissues, placed on silver wire electrodes for electrical stimulation and covered with dental impression material. Partial pressures of O_2 and CO_2 as well as pH of the arterial blood were measured every 1–2 h. End-tidal levels of CO_2 were monitored on-line using a fast-response CO_2 analyser (model Capstar-100, CWE Inc., Ardmore, PA, USA) and kept at 4–5% by adjusting tidal volume and respiratory frequency. The body temperature was maintained with a servo-controlled heating pad at 37.0 $\pm$ 0.2°C.

ATP and glutamate biosensors

The design and operation of the enzyme-based ATP biosensors used in this study have been described in detail elsewhere (Llaudet *et al.* 2003, 2005; Gourine *et al.* 2005*a*,*b*; Frenguelli *et al.* 2007). The ATP sensors comprised two enzymes, glycerol kinase and glycerol-3-phosphate oxidase, entrapped within a matrix around a fine Pt wire of 50 or 100 μm in diameter and 1 mm long.

The glutamate biosensor contained glutamate oxidase entrapped within a matrix around Pt wire (diameter 50 μm, length 1 mm). Glutamate oxidase converts glutamate to α-ketoglutarate with the production of NH_3 and H_2O_2. Like the ATP biosensor, the glutamate sensor thus relies on the amperometric detection of H_2O_2 produced within the thin enzymatic layer around the microelectrode tip. Both the ATP and glutamate biosensors respond rapidly to changes in analyte concentration achieving a 10–90% response time of less than 10 s (Fig. 1*A*) (Llaudet *et al.* 2005).

Electrochemical sensors can respond not only to the analyte of interest, but also to any other electro-active species in the milieu such as ascorbate, urate or catecholamine transmitters. The biosensors used in this study had an internal permselective layer of poly-phenylenediamine that greatly increased their selectivity for the analyte of interest *versus* electroactive species (Masse *et al.* 2007; Frenguelli *et al.* 2007).

Nevertheless, in all experiments we controlled for the release of these 'non-specific' electroactive interferents by using a dual recording configuration: in addition to an ATP or glutamate sensor that was inserted into one side of the medulla, a null sensor lacking enzymes but otherwise identical in size and shape was inserted into an equivalent position on the other side of the medulla (Fig. 1*B*).

Sensors were calibrated *in vitro* immediately prior and after the recordings (some 1–2 h later) to test whether

they retained sensitivity. During the recordings, ATP and glutamate sensors lost on average ∼70% and ∼50% of their initial sensitivities, respectively. To convert changes in sensor current to changes in analyte concentrations, the mean of the initial and final calibrations was used. Note that this conversion assumes that the entire surface are of the sensor is in contact with the sites releasing ATP and glutamate. This is unlikely to be the case (see Results) and the concentrations reported below are likely to substantially underestimate the actual amounts of ATP and glutamate released. Nevertheless, this presentation of sensor current in units of concentration allows for differences in sensitivity between the biosensors.

Measurements of the lung inflation-induced changes in ATP and glutamate concentrations in the NTS

The sensors were connected to a MicroC potentiostat (WPI, Sarasota, FL, USA) and held on a stereotaxic micromanipulator. The sensors were aligned with the obex and placed into the NTS sites (0.3–0.5 mm rostral, 1.0 mm lateral and 0.6–1.0 mm ventral of obex) where central terminals of pulmonary SARs terminate (Fig. 1*B* and *C*) (Bonham & McCrimmon, 1990; Wasserman *et al.* 2000). The identical placement of the ATP, glutamate sensors and respective null sensors was achieved by aligning them to the obex and by means of the vernier scale of the manipulator. Once the sensors were placed, the exposed area of the brainstem and both sensors were covered with modified Bulmer's buffer (to provide glycerol for the operation of the ATP biosensor) and a period of 20–30 min was allowed for the biosensors to polarize to their operating potential (+500 mV with respect to Ag–AgCl).

To determine the nature of the rhythmic signals recorded by the ATP and glutamate biosensors, the following tests were performed: (i) induction of central apnoea by mechanical hyperventilation (reducing blood and brain levels of P_{CO_2}) to determine dependence of the rhythmic ATP release upon the central respiratory drive; (ii) reversible blockade of the vagus nerve conductance (including pulmonary SARs conductance) by topical application of the local anaesthetic lidocaine (1%) to determine the dependence of the rhythmic ATP and glutamate releases upon vagal nerve input; (iii) application of high concentrations of EAA receptor antagonist

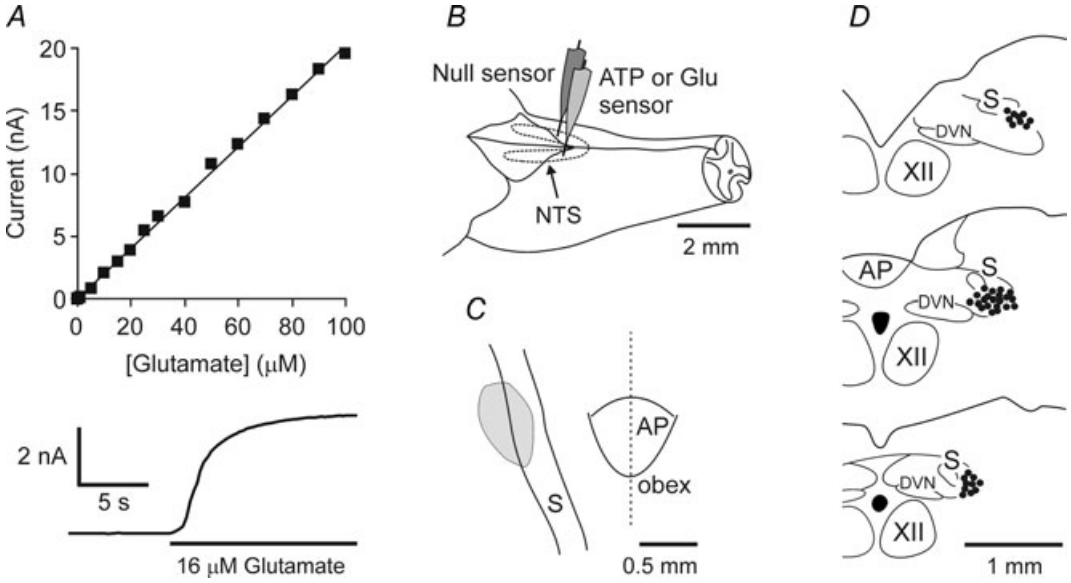

Figure 1. Performance of the glutamate biosensors, sensor placement in the nucleus of the solitary tract (NTS) and locations of the second order relay neurones which receive monosynaptic inputs from the slowly adapting pulmonary stretch receptor afferents
A, calibration curve of the glutamate biosensor demonstrating linearity of glutamate detection in concentrations from 1 μM to 100 μM and an expanded portion of the calibration trace demonstrating the fast response characteristics of the biosensor. Change-over of the solution in the calibration chamber was not a step change. It would take a few seconds for glutamate to reach the desired concentration. Note that the sensor responds immediately when glutamate solution is starting to enter the chamber. *B*, schematic showing the sensor placement in the NTS. A dual recording configuration of ATP (or glutamate) sensor placed upon one side of the medulla along with a null sensor that was placed in an equivalent position on the contralateral side was used (see main text for details). *C*, grey area depicts the region from which biosensor recordings were made. *D*, locations of the 42 pump cells recorded. The locations of the recording sites were identified by ionophoretic deposition of Pontamine Sky Blue dye. XII, hypoglossal nucleus. AP, area postrema. DVN, dorsal motor nucleus of the vagus nerve, S, solitary tract. Anatomical structures are indicated according to the classification of Paxinos & Watson (1986).

kynurenic acid (5 mM) or GABA (100 mM) on the exposed dorsal surface of the brainstem to determine the dependence of the signals recorded with the ATP sensor upon NTS neuronal activities; and (iv) electrical stimulation of the vagus nerve (1 ms pulses, 0.5 mA, 100 Hz for 250 ms) to determine whether it could trigger release of ATP in the NTS (stimulation of the vagus nerve at this high frequency is believed to mimic lung inflation in opposition to low-frequency stimulation which mimics lung deflation (Kato *et al.* 2004)).

At the end of the experiment the animals were killed humanely by an overdose of pentobarbitone sodium (200 mg kg^{-1}, I.V.), the brains were removed and the locations of the recording sites were identified histologically and mapped using a stereotaxic atlas (Paxinos & Watson, 1986). Histological analysis of the sensor placements confirmed that recording sites were within the targeted region of the NTS.

Recordings of the NTS neurones

Extracellular single-unit recordings and ionophoretic application of drugs were made using 5-barrelled microelectrodes (tip diameter 1–3 μm, resistance 5–15 MΩ). The recorded signal was amplified ($\times$10 000) and filtered (0.5–1.5 kHz). The recording barrel of the microelectrode contained NaCl (4 M). The other barrels of the microelectrode contained ATP (20 mM, pH 8.0), P2 receptor blocker suramin (20 mM, pH 8.0) or pyridoxal-5′-phosphate-6-azophenyl-2′,4′-disulphonic acid (PPADS, 100 μM, pH 8.0), EAA receptor antagonist kynurenic acid (100 mM, pH 8.0) and Pontamine Sky Blue dye (2% in 0.2 M sodium acetate). All the drugs were retained in the barrels by application of 15 nA current and ejected using negative currents. The concentrations of ATP, suramin and PPADS have been chosen based on the results of the previous studies that investigated the effects of these compounds on the activity of the ventral medullary respiratory neurones (Ralevic *et al.* 1999; Thomas & Spyer, 2000; Gourine *et al.* 2003). All drugs were from Sigma (Poole, UK).

Pump cells were identified based on the following criteria (Ezure *et al.* 1998; Miyazaki *et al.* 1998, 1999; Ezure & Tanaka, 2000): (i) discharge pattern phase-locked to lung inflation; (ii) inspiratory inhibition; (iii) slowly adapting discharge in response to maintained lung inflation; (iv) monosynaptic activation by electrical stimulation of the ipsilateral vagus nerve (latencies < 3 ms). Although not specifically targeted, other NTS neurones with rhythmic respiratory-related discharge were also recorded and their responses to ionophoretic application of ATP were determined. These included inspiratory Iβ neurones (identification criteria: (i) discharge during the inspiratory phase of the respiratory cycle; (ii) monosynaptic activation by electrical stimulation of the vagus nerve; and (iii) tonic maintained discharge during lung inflation), Iα neurones (the rest of the NTS neurones with inspiratory-related discharge which is not affected by lung inflation or deflation) and deflation-sensitive neurones (Ezure & Tanaka, 2000).

Once a steady firing rate of the neurone had been established, drugs were applied ionophoretically (Neurophore, Medical Systems Corp., NY, USA). Effects of ATP, suramin and PPADS applied with the currents of 25 and 50 nA for 40 s were determined. The effects of P2 receptor antagonist suramin and EAA receptor antagonist kynurenic acid applied individually or simultaneously on the activity of pump cells were also recorded and compared. Recording sites were marked by ionophoretic deposition of Pontamine Sky Blue dye (500 nA; 10 min). At the end of the experiment the animal was terminally anaesthetized with pentobarbitone sodium (200 mg kg^{-1}, I.V.) and was perfused transcardially with 100 ml of heparinized saline followed by 200 ml of 4% paraformaldehyde in 0.1 M phosphate buffer (pH 7.4). Brains were removed, postfixed, sectioned serially (100 μm) and counterstained with Neutral Red. Recording sites were visualized using a light microscope and mapped using a stereotaxic atlas (Fig. 1*D*) (Paxinos & Watson, 1986).

Microinjections into the NTS

The rats were prepared as described above (see Surgical procedure). A three-barrelled glass micropipette (tip size 20–25 μm) was placed in the NTS region where SARs terminate (0.3–0.5 mm rostral, 1.0 mm lateral and 0.6–1.0 mm ventral of obex). The barrels of the micropipette contained ATP (20 mM, pH 7.4), vehicle (aCSF consisted of (mM): 124 NaCl, 3.3 KCl, 2.4 $CaCl_2$, 1.3 $MgSO_4$, 26 $NaHCO_3$, 1.2 KH_2PO_4 and 10 D-glucose; saturated with 95% O_2–5% CO_2; pH 7.4) and Pontamine Sky Blue dye (2% in 0.2 M sodium acetate). The injections were made using pressure over a period of 5–10 s and were monitored using a dissecting microscope with a calibrated micrometer eyepiece. First, unilateral microinjection of aCSF (50 nl) was made to observe the pressure effect. Then, the effect of ATP microinjected into the NTS on baseline respiratory activity was determined. The sites of microinjections were marked by injection of Pontamine Sky Blue dye, identified histologically and mapped using a stereotaxic atlas (Paxinos & Watson, 1986).

Data analysis

Recordings were processed using a Power 1401 interface and analysed using Spike 2 software (Cambridge Electronic Design, Cambridge, UK). Rhythmic changes in ATP and glutamate levels are presented as both raw data and means $\pm$ S.E.M. of peak (in nM) increases in concentrations. The amplitude of ATP and glutamate

signals before and after blockade of the vagus nerve conductance, kynurenic acid or GABA applications on the dorsal surface of the medulla oblongata were compared using Student's paired t test. Neuronal single-unit discharge is expressed as raw data or rate histograms after discrimination of the activity with a window discriminator. Baseline firing was assessed by averaging firing rate during the active phase of the neurone over 10–20 respiratory cycles prior to the application of drugs. Neuronal discharge frequencies before and during applications of drugs were compared using Student's paired t test. A value of $P < 0.05$ was considered to be significant.

Results

Rhythmic ATP release in the NTS

ATP microelectrode biosensors placed into the area of the NTS where SARs terminate (Fig. 1*C*) detected a rhythmic signal that was phase locked to changes in tracheal pressure (a measure of lung inflation) (Fig. 2*A* and *B*). This signal had a mean amplitude of 11.7 ± 1.3 pA ($n = 10$). No such rhythmic signal was detected by the 'null' sensors that lacked enzymes in the polymer coating or by the ATP biosensors placed outside this circumscribed area (Fig. 2*C*). This rhythmic signal recorded by the ATP biosensors within the NTS was equivalent to a peak change in ATP concentration of 61 ± 8 nM ($n = 10$). Peak increase in ATP level was observed 60 ± 16 ms ($n = 10$) after the peak increase in tracheal pressure (see Fig. 4*B*). There was a strong correlation ($R^2 = 0.81$, $P = 0.014$) between the amplitude of the recorded rhythmic signal and the sensitivity of the ATP biosensors. Given that ATP seems to be released from a circumscribed area of the NTS it is unlikely that the entire surface area of the biosensor is in contact with the releasing tissue. This estimate of the change in ATP concentration is therefore likely to be an underestimate of the true change (see Methods).

Rhythmic ATP release in the NTS does not depend upon inspiratory activity

To test whether the rhythmic ATP release depended upon the central respiratory drive, central apnoea was

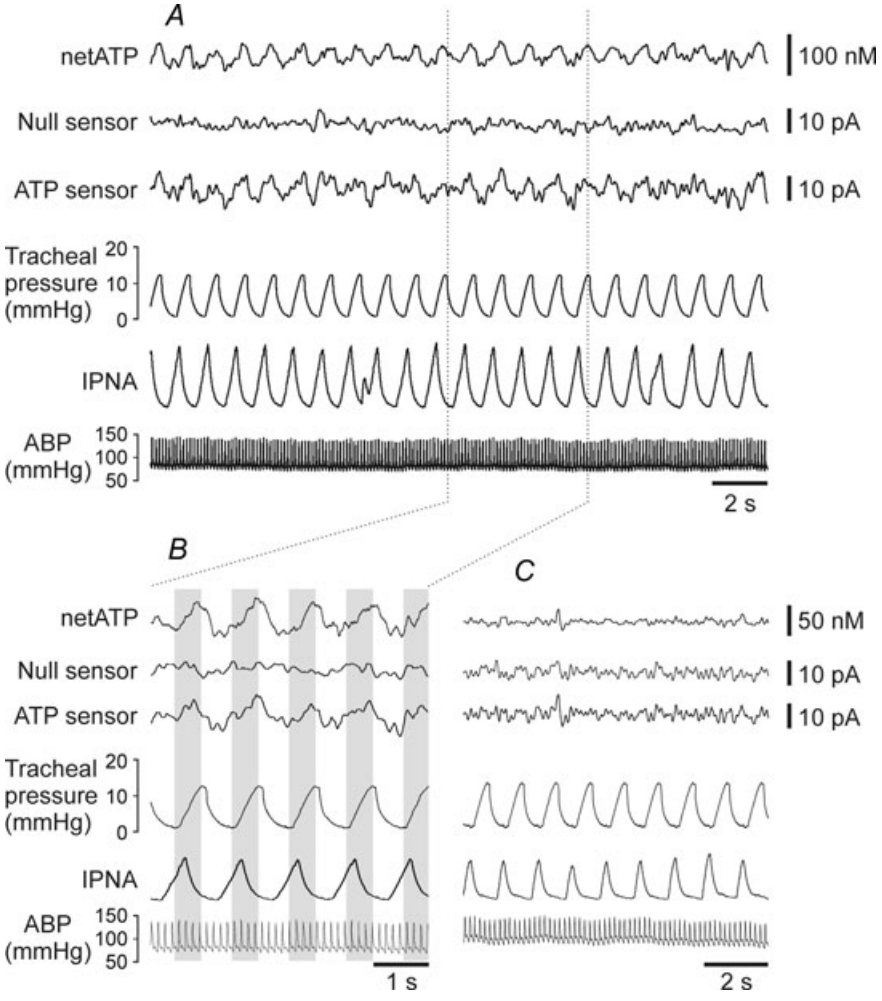

Figure 2. Rhythmic ATP release in the NTS
A, representative raw data illustrating records of the arterial blood pressure, phrenic nerve activity, tracheal pressure, null and ATP sensor currents. The sensors were placed into the NTS area where slowly adapting pulmonary stretch receptor afferents terminate. 'netATP' trace represents difference in sensor signal between ATP and null sensors. *B*, an expanded portion of the same record demonstrating rhythmic ATP release phase locked to changes in tracheal pressure. *C*, raw data illustrating records of the arterial blood pressure, phrenic nerve activity, tracheal pressure, null and ATP sensor currents when the sensors are placed into the commissural NTS. ABP, arterial blood pressure; IPNA, integrated phrenic nerve activity (arbitrary units).

induced by mechanical hyperventilation to reduce blood and brain levels of P_{CO_2} below the apnoeic threshold (Fig. 3). Mechanical hyperventilation first greatly reduced the amplitude of the phrenic nerve bursts; however, the rhythmic ATP signal was enhanced (in line with the greater lung inflation) and remained phase locked to changes in tracheal pressure (Fig. 3). Furthermore, the dependence on lung inflation, as opposed to centrally generated respiratory activity, was confirmed by continuing hyperventilation to the point where apnoea was induced, but rhythmic ATP release, phase locked to changes in tracheal pressure, remained (Fig. 3).

Rhythmic ATP release in the NTS is dependent upon vagal nerve afferent input

To determine whether this rhythmic ATP release requires vagal nerve input, the nerve was exposed to allow reversible blockade of the conductance (including pulmonary SARs conductance) by topical application of local anaesthetic. After recording a control period of rhythmic ATP release, lidocaine (1% in saline) was applied to the ipsilateral vagus nerve. This treatment immediately increased the duration of the phrenic nerve discharge to that typically observed in a vagotomized animal and almost completely abolished the rhythmic ATP release (Fig. 4). After a period of washing (10–15 min) the nerve with saline, full recovery of the ATP signal and phrenic nerve discharge pattern were achieved (Fig. 4).

Rhythmic ATP release in the NTS is not affected by the blockade of EAA receptors or activation of GABA receptors

The EAA receptor antagonist kynurenic acid or GABA were applied in high concentrations (5 and 100 mM, respectively) to the exposed dorsal surface of the brainstem. Both treatments resulted in a significant alteration of autonomic activity, as evident from the reduced respiratory activity and marked changes (either decrease evoked by GABA or increase evoked by kynurenic acid) in blood pressure (Fig. 5*A*). However, the amplitude of the rhythmic ATP release phase-locked with lung inflation cycle was unchanged (Fig. 5*B*).

Electrical stimulation of the vagus nerve evokes ATP release in the NTS

After cutting the vagus nerve (to eliminate rhythmic lung inflation-induced ATP release in the NTS), its central end was stimulated electrically to determine whether it could trigger release of ATP. Trains of electrical stimuli were delivered at a rate slightly higher than the ventilator rate (Fig. 5*C*) to determine whether sensor dynamics and sensitivity were sufficient to accurately follow rapid phasic changes in ATP concentration. It was found that electrical stimulation of the vagus nerve reliably evoked ATP release in the NTS area where pulmonary SARs terminate (Fig. 5*C*).

Rhythmic glutamate release in the NTS: dependence upon vagal nerve afferent input

Previous reports have presented strong evidence for a role for glutamate in mediating the transmission from the SARs to the NTS second order relay neurones (Bonham *et al.* 1993; Zhang & Mifflin, 1995; Miyazaki *et al.* 1999). To confirm the role of glutamate, and compare release of glutamate in the NTS during lung inflation cycle with that of ATP, we devised a glutamate biosensor (Fig. 1*A*, see Methods) and placed it within the NTS at the locations where we had previously seen rhythmic ATP release (Fig. 1*B* and *C*).

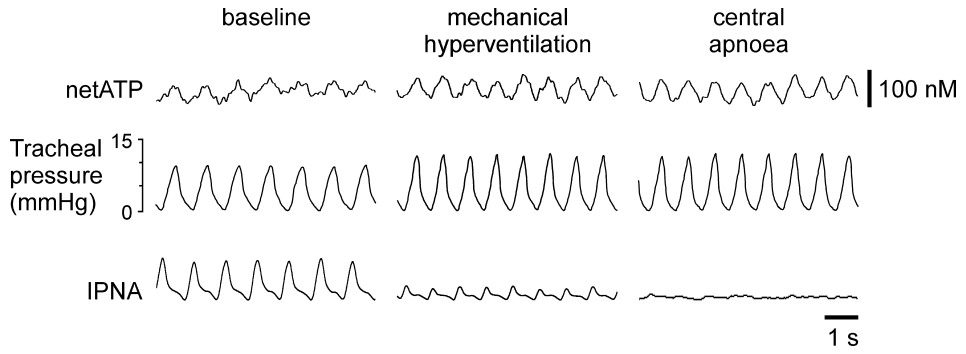

Figure 3. Rhythmic ATP release in the NTS does not depend upon central respiratory drive
Representative raw data showing recordings of the phrenic nerve activity, tracheal pressure and difference in current between ATP and null sensors in basal conditions and during mechanical hyperventilation resulting in central apnoea (arterial P_{CO_2} and end-tidal CO_2 below apnoeic threshold). IPNA, integrated phrenic nerve activity (arbitrary units).

A signal was recorded on the glutamate biosensors (but not on the 'null' sensors) that was similar to that detected by the ATP biosensors: rhythmic release phase locked to changes of tracheal pressure (Fig. 6*A*). The amplitude of the signal was 8.8 ± 0.8 pA ($n = 6$), and this was equivalent to a rhythmic change in glutamate concentration of 39.8 ± 3.5 nM ($n = 6$) in magnitude. Peak increase in glutamate level was observed 93 ± 17 ms ($n = 6$) after the peak increase in tracheal pressure. This estimate of glutamate release is very likely an underestimate for the same reasons outlined above. However, the amplitude of the recorded rhythmic signal correlated very strongly ($R^2 = 0.76$, $P = 0.005$) with the sensitivity of the glutamate biosensors determined *in vitro*.

To test the dependence of glutamate release in the NTS on the vagal nerve input, we once again utilized reversible blockade of this nerve by topical application of lidocaine. Lidocaine (1% solution) application on the cervical vagus nerve resulted in a significant blockade of the rhythmic glutamate release (Fig. 6*B–D*) – the effect similar to that observed when ATP release was studied (Fig. 4). Kynurenic acid (5 mM; $n = 3$, data not shown) or P2 receptor antagonist PPADS (1 or 10 mM; $n = 4$, Fig. 6*D*) applied on the dorsal surface of the brainstem had no effect on the amplitude of rhythmic glutamate release in the NTS.

ATP induces an increase in discharge of the NTS second order relay neurones that receive SARs input

The responses of 12 NTS pump cells were tested to ionophoretical application of ATP. ATP induced a significant (on average by ~60%) increase in firing frequency of every single pump cell recorded (Fig. 7*A–C*). This increase in the discharge frequency in response to ATP was observed only during the active phase of the neurone; firing was not induced by ATP during the phase of the inspiratory inhibition of the pump cells (Fig. 7*A*). All Iβ neurones tested ($n = 4$) also increased their firing in response to ATP by the same extent (Fig. 7*C*). In contrast, none of the recorded Iα neurones ($n = 8$) and deflation-sensitive neurones ($n = 6$) responded to

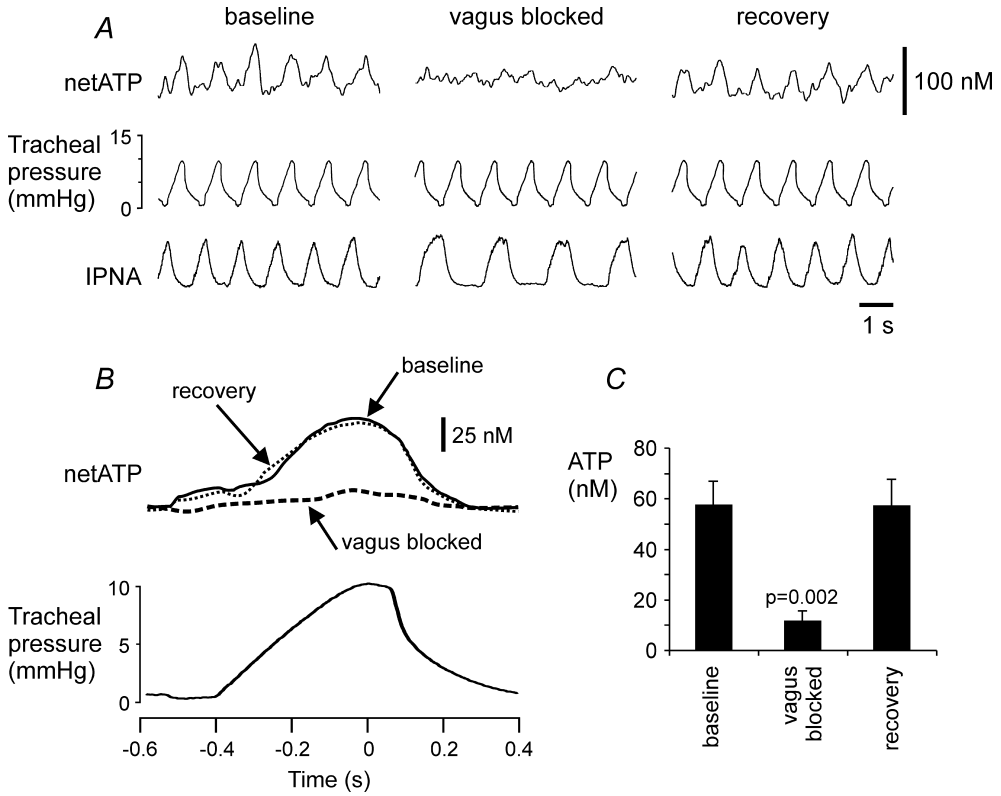

Figure 4. Rhythmic ATP release in the NTS is dependent upon vagal nerve afferent input
A, representative raw data showing recordings of the phrenic nerve activity, tracheal pressure and difference in current between ATP and null sensors in basal conditions and during reversible blockade of the vagus nerve conductance by topical application of lidocaine (1% in saline). *B*, results are presented as the averages of the netATP trace for 60 inflation–deflation cycles triggered from the peak of tracheal pressure increase before, during and after lidocaine application on the vagus nerve (ipsilateral to the ATP sensor placement in the NTS). *C*, mean amplitudes of the ATP signal before, during and after blockade of the vagus nerve conductance ($n = 6$). IPNA, integrated phrenic nerve activity (arbitrary units).

microionophoretic application of ATP with changes in their discharge (Fig. 7*C*).

ATP application into the NTS evokes apnoea

In six anaesthetized and artificially ventilated animals, microinjection of ATP (20 mM, 50 nl) into the NTS site where SARs terminate induced immediate and prolonged cessation of the respiratory activity (Fig. 7*D*). A period of ATP-induced apnoea lasted 39 ± 4 s.

Both P2 and glutamate receptors mediate excitation of the second order relay neurones

As a final test of the respective roles of glutamate and ATP release in the NTS, the effects of EAA and P2 receptor antagonists on firing of the second order relay pump neurones were examined (Fig. 8). To reduce the spread of the drugs to neighbouring neurones, the ionophoretic currents were kept as low as possible. It was found that PPADS (100 μM, 50 nA), suramin (20 mM, 50 nA) as well as kynurenic acid (100 mM, 50 nA) reduced discharge of the NTS pump cells by 16% ($P < 0.001$, $n = 16$), 22% ($P < 0.0001$, $n = 16$) and 28% ($P < 0.0001$, $n = 15$), respectively (Fig. 8*C*). In contrast, discharge of Iα neurones was not affected by either PPADS ($n = 4$) or suramin ($n = 5$), although kynurenic acid had a small but significant effect, reducing firing of Iα cells by 10% ($P < 0.01$, $n = 5$, Fig. 8*C*). In a further nine pump neurones, the effects of suramin and kynurenic acid applied either individually or in combination were studied. Suramin and kynurenic acid applied using a smaller current of 25 nA reduced firing of the pump cells by 13% ($P < 0.001$, $n = 9$) and 14% ($P < 0.001$, $n = 9$), respectively (Fig. 8*B* and *D*). When these agents were applied simultaneously pump cell's discharge was reduced by 37% ($P < 0.0001$) (Fig. 8*D*). However, the decrease in discharge during simultaneous application of suramin and kynurenic acid was not significantly greater ($P = 0.078$) than the sum of the effects of each drug applied alone,

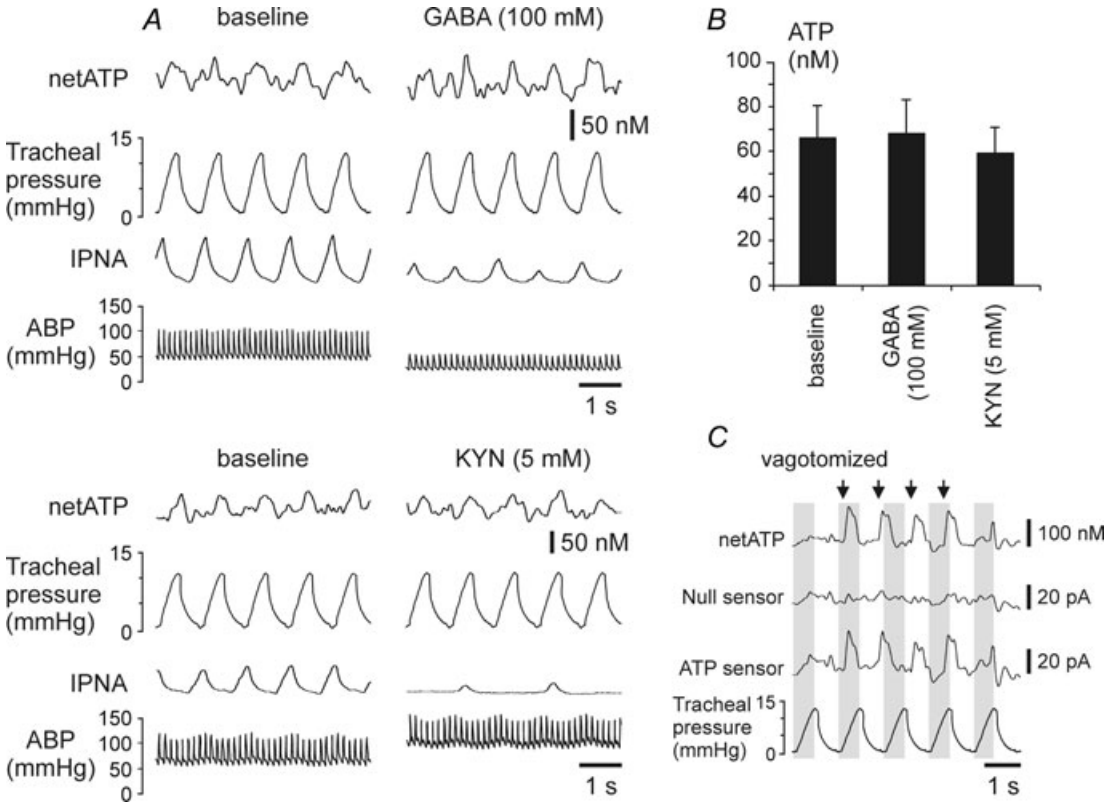

Figure 5. ATP release in the NTS is not affected by the blockade of excitatory amino acid receptors or activation of GABA receptors and can be evoked by electrical stimulation of the vagus nerve
A, raw data showing recordings of the arterial blood pressure, phrenic nerve activity, tracheal pressure and difference in current between ATP and null sensors in basal conditions and during applications of EAA receptor antagonist kynurenic acid (KYN) or GABA on the exposed dorsal surface of the brainstem. *B*, mean amplitudes of the rhythmic ATP signal following applications of kynurenic acid or GABA on the dorsal surface of the brainstem ($n = 4$). *C*, electrical stimulation of the vagus nerve triggers release of ATP in the NTS. Arrows indicate the onset of 250 ms stimulation period. ABP, arterial blood pressure; IPNA, integrated phrenic nerve activity (arbitrary units).

suggesting an additive action between ATP and glutamate on the activity of the NTS pump cells. (In three neurones at the end of the recordings, suramin and kynurenic acid were applied simultaneously using 50 nA currents (Fig. 8*B*). Since these applications were tested in 3 out of 9 cells we were unable to compare the effects observed with the rest of the data.)

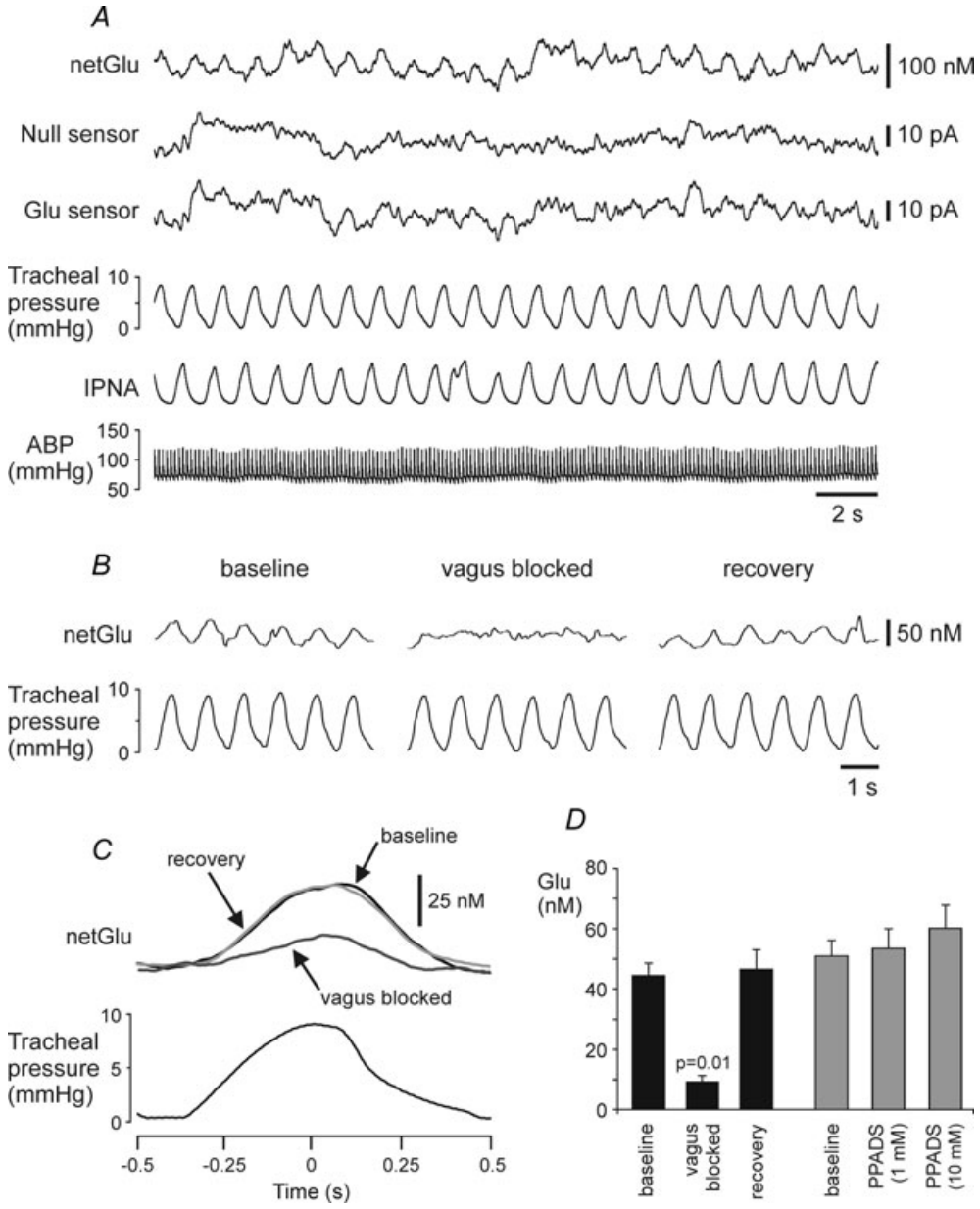

Figure 6. Rhythmic glutamate release in the NTS. Dependence upon vagal nerve afferent input
A, raw data illustrating records of the arterial blood pressure, phrenic nerve activity, tracheal pressure, null and glutamate sensor currents. The sensors were placed into the NTS area where slowly adapting pulmonary stretch receptor afferents terminate. 'netGlu' trace represents difference in sensor signal between glutamate and null sensors. *B*, raw data showing recordings of the tracheal pressure and difference in current between glutamate and null sensors in basal conditions and during reversible blockade of the vagus nerve conductance by topical application of lidocaine (1% in saline). *C*, results are presented as the averages of the netGlu trace for 60 inflation–deflation cycles triggered from the peak of tracheal pressure increase before, during and after lidocaine application on the vagus nerve (ipsilateral to the glutamate sensor placement in the NTS). *D*, black columns: mean amplitudes of the rhythmic glutamate signal before, during and after blockade of the vagus nerve conductance ($n = 5$). Grey columns: mean amplitudes of the rhythmic glutamate signal in basal conditions and following application of pyridoxal-5′-phosphate-6-azophenyl-2′,4′-disulphonic acid (PPADS) on the exposed dorsal surface of the brainstem ($n = 4$). ABP, arterial blood pressure. IPNA, integrated phrenic nerve activity (arbitrary units).

Discussion

The data obtained in the present study suggest that ATP and glutamate are released in the NTS from the central terminals of the slowly adapting lung stretch receptor afferents, activate the second-order relay neurones and hence mediate the Breuer–Hering inflation reflex.

Technical considerations

In our previous studies in anaesthetized and conscious rats and rabbits we used biosensors to measure changes in ATP and adenosine concentrations in the hypothalamus and the brainstem (Gourine *et al.* 2002, 2005*a*,*b*, 2007; Dale *et al.* 2002). These studies described relatively slow (developing over several seconds and minutes) changes in

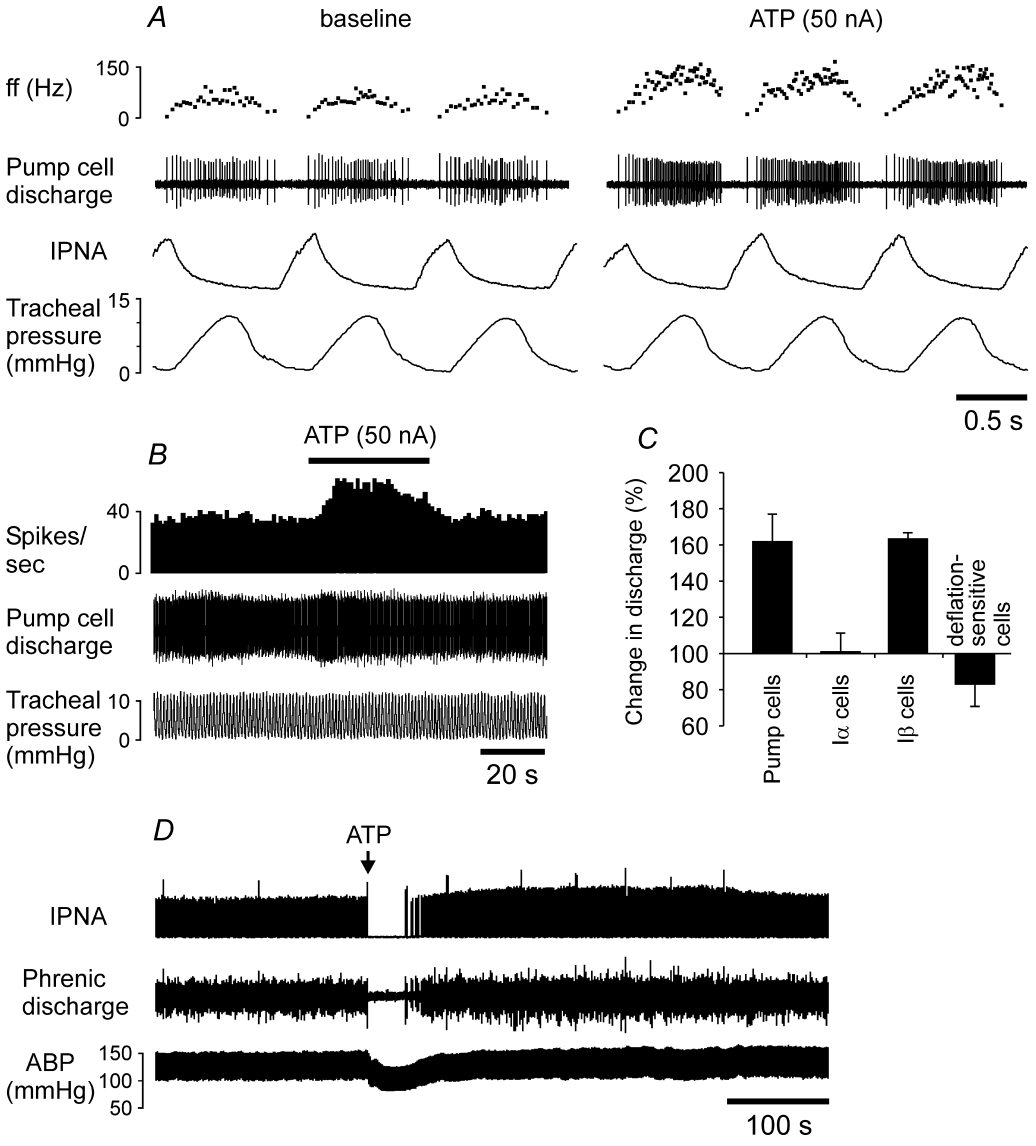

Figure 7. ATP induces an increase in discharge of the NTS pump cells and evokes central apnoea when injected into the NTS

A, raw data illustrating the response of the NTS pump neurone to microionophoretic application of ATP (20 mM). *B*, time-condensed record of the firing rate of the same neurone. Black horizontal bar indicates timing of ATP application. *C*, summary data of peak change in discharge of the NTS rhythmic neurones induced by microionophoretic application of ATP (20 mM, 50 nA). Numbers of neurones in each group are given in the main text (see Results). *D*, raw data illustrating the effect of ATP (20 mM, 50 nl) on the respiratory activity and arterial blood pressure when microinjected unilaterally into the NTS site where SARs terminate. ABP, arterial blood pressure. ff, instantaneous firing frequency. IPNA, integrated phrenic nerve activity (arbitrary units).

analyte concentrations during physiological responses to systemic hypoxia, hypercapnia or inflammation. Here, we have measured rapid rhythmic peaks of ATP and glutamate release at the first central synapses of pulmonary mechanoafferents.

Biosensors placed into the brain tissue *in vivo* are prone to non-specific detection of either mechanical (movement of the brain due to the ventilation of the lungs) or chemical (release of some electroactive interferents) artifacts. This is especially important when we record relatively small signals like those detected in the present study. These signals appear to be genuine rhythmic changes in ATP and glutamate levels for several reasons. First, in each experiment, null sensors lacking essential

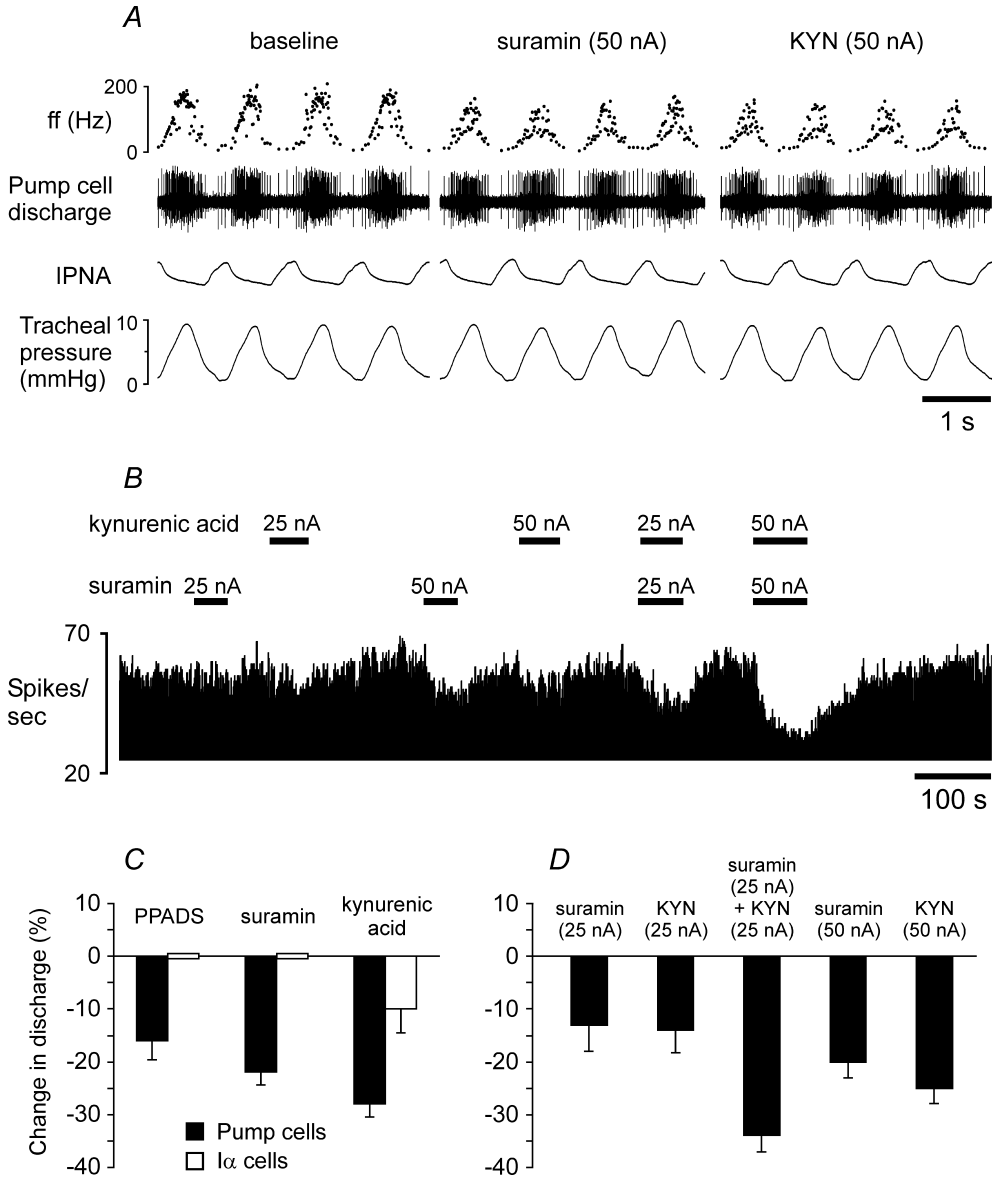

Figure 8. Blockade of ATP receptors and/or excitatory amino acid receptors decreases discharge of the NTS pump cells

A, raw data illustrating the response of the NTS pump neurone to microionophoretic application of P2 receptor antagonist suramin (20 mM) or EAA blocker kynurenic acid (KYN, 100 mM). *B*, time-condensed record of the firing rate of the same neurone illustrating its responses to suramin (20 mM) and kynurenic acid (100 mM) applied using the currents shown. Black horizontal bars indicate timings of suramin or kynurenic acid applications. *C*, summary data of changes in discharge of the NTS pump cells and Iα neurones evoked by microionophoretic applications of PPADS (100 μM, 50 nA), suramin (50 nA) or kynurenic acid (50 nA). Numbers of neurones in each group are given in the main text (see Results). *D*, summary data of changes in discharge of the NTS pump neurones ($n = 9$) evoked by suramin and kynurenic acid applied either individually or in combination.

detecting enzymes in the polymer layer were placed into an equivalent position on the contralateral site of the medulla. No rhythmic signal was detected by these control sensors. Second, rhythmic signals were not detected by either ATP or glutamate biosensors when placed outside the circumscribed NTS area where SARs terminate (Bonham & McCrimmon, 1990). These two observations eliminate several types of possible artifacts, e.g. that the sensors were: (i) picking up a field potential; (ii) measuring non-specific electroactive interferents; or (iii) the signals were due to mechanical movement of the tissue. Third, there was a strong correlation between the amplitude of the rhythmic signal and the sensitivity of the biosensors.

This dependence of signal amplitude on biosensor sensitivity strongly indicates that the rhythmic signals recorded were indeed due to rhythmic release of ATP or glutamate. By extension, these results indicate that the speed of the biosensor response is sufficient to rapidly follow rhythmic changes in ATP or glutamate concentrations occurring with the cycle length of ∼1 s. This is not obvious from the presented calibration curve (Fig. 1*A*), since change-over of the solution in the calibration chamber was not a step change and it would take a few seconds for glutamate to reach the desired concentration (note that the sensor responds immediately as the analyte solution is entering the chamber).

Although the evidence obtained leaves little doubt that the signals detected by the ATP and glutamate sensors in the NTS represent rhythmic changes in ATP and glutamate levels, the values of peak ATP and glutamate releases reported above are likely to substantially underestimate the actual amounts released. First, as discussed above, conversion of sensor current to changes in analyte concentrations assumes that the entire surface of the sensor is in contact with the sites releasing ATP and glutamate. This is unlikely to be the case. Second, the measured rhythmic changes in ATP and glutamate concentrations may represent only a small fraction of what is actually released due to high activities of ectonucleotidases rapidly breaking down ATP and extremely powerful glutamate re-uptake mechanisms. Nevertheless, values of peak ATP and glutamate releases provide important information regarding changes in ATP and glutamate levels in the vicinity of the sensor and allow determination of the effect of a given treatment (i.e. blockade of the vagus nerve conductance) on their release.

The glutamate signal reaches a peak significantly later following the peak increase in tracheal pressure (93 ± 17 ms, $n = 6$) than the ATP signal (60 ± 16 ms, $n = 10$, $P < 0.05$). This difference in dynamics could arise from three possible sources: (i) differences in ATP and glutamate biosensor dynamics; (ii) differences in the dynamics of ATP and glutamate release; or (iii) differences in the speed of ATP and glutamate diffusion from their sites of release to the biosensor. As the dynamics of the ATP and glutamate biosensors are very similar, we think the first explanation is unlikely. Since our evidence suggests that ATP and glutamate are both released from the SARs central terminals, we think that the second explanation is also unlikely. Instead we favour the notion that diffusion of ATP and glutamate through the neural tissue differs. ATP neurotransmission is terminated by the actions of ectoATPases that break down ATP to ADP and downstream purines (Robson *et al.* 2006). Glutamate transmission is terminated by diffusion away from the synaptic cleft and uptake through high-affinity transporters (Danbolt, 2001). The dynamics of these processes and the distribution of transporters and ectoATPases are likely to be sufficiently different to explain the distinctive dynamics of the ATP and glutamate signals.

Source of rhythmic ATP and glutamate release in the NTS

The ATP and glutamate microelectrode biosensors detected rhythmic signals in the vicinity of the SAR terminals phase-locked to changes in tracheal pressure. This observation does not unambiguously indicate that the central terminals of SARs release ATP and glutamate; they could be released instead by the populations of second-order relay (e.g. pump cells) or other NTS neurones with rhythmic respiratory-related discharge (e.g. Iβ neurones). Three pieces of evidence make these alternatives unlikely.

First, rhythmic ATP release shows independence of the central respiratory activity – the amplitude of the recorded signal was not diminished when central apnoea was induced by mechanical hyperventilation (which would also reduce or abolish the activities of the NTS respiratory neurones). Second, rhythmic ATP and glutamate release requires vagus nerve input – the signals were reversibly abolished during blockade of the vagus nerve conductance by topical application of the local anaesthetic. Third, the amplitudes of the rhythmic ATP and glutamate signals were not affected by high concentrations of kynurenic acid or GABA applied on the dorsal surface of the brainstem – both of these treatments are expected to significantly depress neuronal activities in the dorsal medullary structures, including the NTS (note profound changes in blood pressure and respiratory activity following kynurenic acid or GABA applications, Fig. 5*A*). Our data therefore suggest very strongly that SARs indeed release ATP and glutamate from their central terminals in the NTS.

Roles of ATP and glutamate in mediating the Breuer–Hering inflation reflex

The data obtained in the current study suggest that both ATP and glutamate mediate the Breuer–Hering inflation

reflex at the central terminals of the SARs. Unilateral microinjection of ATP into the NTS site of release produced central apnoea – this mimics the effect of lung inflation on breathing. Similar effects of ATP applications into the intermediate NTS have been described in awake rats and in *in situ* working heart–brainstem rat preparations (Antunes *et al.* 2005*a*,*b*). EAA agonists applied into the same NTS region also cause apnoea and thus similarly mimic the effect of lung inflation (Bonham & McCrimmon, 1990; Bonham *et al.* 1993).

If ATP release mediates excitation from the SARs, it should excite the postsynaptic relay neurones – the pump cells. Indeed, like DL-homocysteic acid (Bonham *et al.* 1993), application of ATP induced a significant increase in firing of all NTS pump cells tested. Interestingly, other NTS neurones (Iβ cells) known to receive monosynaptic input from the SARs (Backman *et al.* 1984) were also excited by ATP, whilst other subpopulations of NTS respiratory cells (e.g. Iα neurones) were not affected. Thus, it appears that in the circumscribed NTS area where SARs terminate, only those neurones that receive inputs from the SARs respond to ATP with increases in their discharge.

Naturally, ATP may have either pre- or(and) post-synaptic actions. It is possible that ATP released from the central terminals of the SARs is acting presynaptically to facilitate release of glutamate from the same/adjacent terminals. This possibility is supported by the evidence obtained previously in *in vitro* experiments showing ATP-induced potentiation of glutamate release from the myelinated afferent terminals in the NTS (Kato & Shigetomi, 2001; Jin *et al.* 2004). However, in this study we found that application of P2 receptor antagonist PPADS in a high concentration on the dorsal surface of the brainstem had no effect on the amplitude of rhythmic glutamate release in the NTS. These data suggest that ATP released from the central terminals of the SARs does not facilitate release of glutamate by presynaptic P2 receptor activation.

Blockade of P2 receptors significantly reduced the rhythmic discharge of the NTS pump cells – an effect similar to that previously reported for EAA receptor antagonists (Bonham *et al.* 1993; Miyazaki *et al.* 1999). We confirmed these earlier observations and demonstrated a significant reduction in pump cell firing during application of kynurenic acid. Previously Miyazaki *et al.* (1999) reported almost complete suppression of pump cells firing by CNQX. In our experiments only ~30% inhibition was achieved when kynurenic acid was applied. However, since we were concerned about the spread of the drugs to the neighbouring neurones, the ionophoretic currents were kept as low as possible. When suramin was applied simultaneously with kynurenic acid the resulting reduction in pump cells firing was not significantly greater than the sum of the effects of each drug applied alone. This suggests an additive action between the ATP- and glutamate-mediated excitation of the pump neurones.

Although our results suggest very strongly that ATP and glutamate are released from the central terminals of the SARs to mediate the Breuer–Hering inflation reflex, there are some data that are difficult to reconcile with our results. Kato *et al.* (2004) demonstrated in rabbits that injection of PPADS into the NTS attenuated respiratory responses evoked by low-frequency stimulation of the vagus nerve (mimicking lung *deflation*), while responses triggered by high-frequency stimulations (mimicking lung *inflation*) were unaffected by PPADS application. This inconsistency between these results and ours may arise from the method of stimulation, and the precise location and doses of PPADS that were used. For example, Kato *et al.* (2004) injected PPADS at a position slightly caudal (obex level, 1.5 mm lateral) from that in our experiments. In any case, the results by Kato *et al.* (2004) suggest that ATP may also mediate transmission in the lung deflation reflex pathway – a very interesting possibility as the respiratory responses to lung inflation or deflation have long been known to utilize distinct afferent pathways (Head, 1889).

Glutamate- and ATP-mediated transmission in central afferent processing

A substantial body of literature demonstrates the importance of glutamatergic transmission in mediating several visceral afferent reflexes, including arterial baroreflexes (Guyenet *et al.* 1987; Kubo & Kihara, 1991; Gordon & Leone, 1991), arterial chemoreflexes (Zhang & Mifflin, 1993, 1995; Vardhan *et al.* 1993; Mizusawa *et al.* 1994) as well as pulmonary stretch receptor reflexes (Bonham *et al.* 1993; Miyazaki *et al.* 1999).

ATP mediates neurotransmission of the parasympathetic (but not respiratory) component of the chemoreceptor reflex (Paton *et al.* 2002). More recently, in the commissural NTS, both glutamate and ATP were proposed to play a role in neurotransmission of the sympathoexcitatory component of the arterial chemoreflex (Braga *et al.* 2007). Our findings now show that ATP signalling and cotransmission with glutamate are even more pervasive in central autonomic functions than had been previously realized.

Although, the data indicate that ATP and glutamate are released in the NTS from the SARs central terminals, the particular details of this co-release remain unclear. A novel vesicular nucleotide transporter has been recently identified (Sawada *et al.* 2008); however, we do not know whether ATP and glutamate are packed and released within the same vesicles or even from the same nerve terminals. SARs are heterogeneous in terms of the firing frequency, threshold, and the firing profile (Sant'Ambrogio, 1982; Widdicombe, 2001). It remains to be determined whether different subsets of SARs release either ATP, glutamate, or both transmitters.

ATP-mediated purinergic signalling in afferent control of breathing

This study contributes to an increasing body of literature indicating that ATP-mediated signalling plays a fundamental role in the mechanisms controlling breathing. In the periphery, in response to a decrease in P_{O_2} (hypoxia) or an increase in $P_{CO_2}/[H^+]$ (hypercapnia), chemosensitive glomus cells of the carotid body (the main peripheral chemosensitive site) release ATP to activate chemoafferent fibres of the carotid sinus nerve which transmit this information to the brainstem respiratory centres (Zhang *et al.* 2000; Rong *et al.* 2003; Zhang & Nurse, 2004). In the ventrolateral medulla, ATP is released following CO_2/H^+-induced activation of central chemoreceptors and acts within the respiratory network to evoke physiologically relevant increases in ventilation (Gourine, 2005; Gourine *et al.* 2005*b*). Thus, it emerges that ATP acts as a common mediator of peripheral and central chemosensory transduction and also contributes to neurotransmission at the first central synapse of the key respiratory reflex – the Breuer–Hering inflation reflex.

References

Adrian ED (1933). Afferent impulses in the vagus and their effect on respiration. *J Physiol* **79**, 332–358.

Antunes VR, Bonagamba LG & Machado BH (2005*a*). Hemodynamic and respiratory responses to microinjection of ATP into the intermediate and caudal NTS of awake rats. *Brain Res* **1032**, 85–93.

Antunes VR, Braga VA & Machado BH (2005*b*). Autonomic and respiratory responses to microinjection of ATP into the intermediate or caudal nucleus tractus solitarius in the working heart-brainstem preparation of the rat. *Clin Exp Pharmacol Physiol* **32**, 467–472.

Backman SB, Anders C, Ballantyne D, Rohrig N, Camerer H, Mifflin S, Jordan D, Dickhaus H, Spyer KM & Richter DW (1984). Evidence for a monosynaptic connection between slowly adapting pulmonary stretch receptor afferents and inspiratory beta neurones. *Pflugers Arch* **402**, 129–136.

Bonham AC, Coles SK & McCrimmon DR (1993). Pulmonary stretch receptor afferents activate excitatory amino acid receptors in the nucleus tractus solitarii in rats. *J Physiol* **464**, 725–745.

Bonham AC & McCrimmon DR (1990). Neurones in a discrete region of the nucleus tractus solitarius are required for the Breuer-Hering reflex in rat. *J Physiol* **427**, 261–280.

Braga VA, Soriano RN, Braccialli AL, de Paula PM, Bonagamba LG, Paton JF & Machado BH (2007). Involvement of L-glutamate and ATP in the neurotransmission of the sympathoexcitatory component of the chemoreflex in the commissural nucleus tractus solitarii of awake rats and in the working heart–brainstem preparation. *J Physiol* **581**, 1129–1145.

Breuer J (1868). Die Selbststeuerung der Athmung durch den Nervus Vagus. *Sber Akad Wiss Wien* **58**, 909–937.

Burnstock G (2007). Physiology and pathophysiology of purinergic neurotransmission. *Physiol Rev* **87**, 659–797.

Dale N, Gourine AV, Llaudet E, Bulmer D, Thomas T & Spyer KM (2002). Rapid adenosine release in the nucleus tractus solitarii during defence response in rats: real-time measurement in vivo. *J Physiol* **544**, 149–160.

Danbolt NC (2001). Glutamate uptake. *Prog Neurobiol* **65**, 1–105.

Edwards FA, Gibb AJ & Colquhoun D (1992). ATP receptor-mediated synaptic currents in the central nervous system. *Nature* **359**, 144–147.

Ezure K & Tanaka I (2000). Identification of deflation-sensitive inspiratory neurons in the dorsal respiratory group of the rat. *Brain Res* **883**, 22–30.

Ezure K, Tanaka I & Miyazaki M (1998). Inspiratory inhibition of pulmonary rapidly adapting receptor relay neurons in the rat. *Neurosci Lett* **258**, 49–52.

Ezure K, Tanaka I, Saito Y & Otake K (2002). Axonal projections of pulmonary slowly adapting receptor relay neurons in the rat. *J Comp Neurol* **446**, 81–94.

Feldman JL & Del Negro CA (2006). Looking for inspiration: new perspectives on respiratory rhythm. *Nat Rev Neurosci* **7**, 232–242.

Feldman JL, Mitchell GS & Nattie EE (2003). Breathing: rhythmicity, plasticity, chemosensitivity. *Annu Rev Neurosci* **26**, 239–266.

Frenguelli BG, Wigmore G, Llaudet E & Dale N (2007). Temporal and mechanistic dissociation of ATP and adenosine release during ischaemia in the mammalian hippocampus. *J Neurochem* **101**, 1400–1413.

Gordon FJ & Leone C (1991). Non-NMDA receptors in the nucleus of the tractus solitarius play the predominant role in mediating aortic baroreceptor reflexes. *Brain Res* **568**, 319–322.

Gourine AV (2005). On the peripheral and central chemoreception and control of breathing: an emerging role of ATP. *J Physiol* **568**, 715–724.

Gourine AV, Atkinson L, Deuchars J & Spyer KM (2003). Purinergic signalling in the medullary mechanisms of respiratory control in the rat: respiratory neurones express the $P2X_2$ receptor subunit. *J Physiol* **552**, 197–211.

Gourine AV, Dale N, Llaudet E, Poputnikov D, Spyer KM & Gourine VN (2007). Release of ATP in the central nervous system during systemic inflammation: Real-time measurement in the hypothalamus of conscious rabbits. *J Physiol* **585**, 305–316.

Gourine AV, Llaudet E, Dale N & Spyer KM (2005*a*). Release of ATP in the ventral medulla during hypoxia in rats: role in hypoxic ventilatory response. *J Neurosci* **25**, 1211–1218.

Gourine AV, Llaudet E, Dale N & Spyer KM (2005*b*). ATP is a mediator of chemosensory transduction in the central nervous system. *Nature* **436**, 108–111.

Gourine AV, Llaudet E, Thomas T, Dale N & Spyer KM (2002). Adenosine release in nucleus tractus solitarii does not appear to mediate hypoxia-induced respiratory depression in rats. *J Physiol* **544**, 161–170.

Guyenet PG, Filtz TM & Donaldson SR (1987). Role of excitatory amino acids in rat vagal and sympathetic baroreflexes. *Brain Res* **407**, 272–284.

Head H (1889). On the regulation of respiration. Part I. Experimental. *J Physiol* **10**, 1–70.

Jin YH, Bailey TW, Li BY, Schild JH & Andresen MC (2004). Purinergic and vanilloid receptor activation releases glutamate from separate cranial afferent terminals in nucleus tractus solitarius. *J Neurosci* **24**, 4709–4717.

Jo YH & Schlichter R (1999). Synaptic corelease of ATP and GABA in cultured spinal neurons. *Nat Neurosci* **2**, 241–245.

Kanjhan R, Housley GD, Burton LD, Christie DL, Kippenberger A, Thorne PR, Luo L & Ryan AF (1999). Distribution of the $P2X_2$ receptor subunit of the ATP-gated ion channels in the rat central nervous system. *J Comp Neurol* **407**, 11–32.

Kato F & Shigetomi E (2001). Distinct modulation of evoked and spontaneous EPSCs by purinoceptors in the nucleus tractus solitarii of the rat. *J Physiol* **530**, 469–486.

Kato F, Shigetomi E, Yamazaki K, Tsuji N & Takano K (2004). A dual-role played by extracellular ATP in frequency-filtering of the nucleus tractus solitarii network. *Adv Exp Med Biol* **551**, 151–156.

Khakh BS & North RA (2006). P2X receptors as cell-surface ATP sensors in health and disease. *Nature* **442**, 527–532.

Kubin L, Alheid GF, Zuperku EJ & McCrimmon DR (2006). Central pathways of pulmonary and lower airway vagal afferents. *J Appl Physiol* **101**, 618–627.

Kubo T & Kihara M (1991). Unilateral blockade of excitatory amino acid receptors in the nucleus tractus solitarii produces an inhibition of baroreflexes in rats. *Naunyn Schmiedebergs Arch Pharmacol* **343**, 317–322.

Llaudet E, Botting NP, Crayston JA & Dale N (2003). A three-enzyme microelectrode sensor for detecting purine release from central nervous system. *Biosens Bioelectron* **18**, 43–52.

Llaudet E, Hatz S, Droniou M & Dale N (2005). Microelectrode biosensor for real-time measurement of ATP in biological tissue. *Anal Chem* **77**, 3267–3273.

Masse K, Bhamra S, Eason R, Dale N & Jones EA (2007). Purine-mediated signalling triggers eye development. *Nature* **449**, 1058–1062.

Miyazaki M, Arata A, Tanaka I & Ezure K (1998). Activity of rat pump neurons is modulated with central respiratory rhythm. *Neurosci Lett* **249**, 61–64.

Miyazaki M, Tanaka I & Ezure K (1999). Excitatory and inhibitory synaptic inputs shape the discharge pattern of pump neurons of the nucleus tractus solitarii in the rat. *Exp Brain Res* **129**, 191–200.

Mizusawa A, Ogawa H, Kikuchi Y, Hida W, Kurosawa H, Okabe S, Takishima T & Shirato K (1994). *In vivo* release of glutamate in nucleus tractus solitarii of the rat during hypoxia. *J Physiol* **478**, 55–66.

Pankratov Y, Castro E, Miras-Portugal MT & Krishtal O (1998). A purinergic component of the excitatory postsynaptic current mediated by P2X receptors in the CA1 neurons of the rat hippocampus. *Eur J Neurosci* **10**, 3898–3902.

Pankratov Y, Lalo U, Krishtal O & Verkhratsky A (2002). Ionotropic P2X purinoreceptors mediate synaptic transmission in rat pyramidal neurones of layer II/III of somato-sensory cortex. *J Physiol* **542**, 529–536.

Pankratov Y, Lalo U, Krishtal O & Verkhratsky A (2003). P2X receptor-mediated excitatory synaptic currents in somatosensory cortex. *Mol Cell Neurosci* **24**, 842–849.

Pankratov Y, Lalo U, Verkhratsky A & North RA (2006). Vesicular release of ATP at central synapses. *Pflugers Arch* **452**, 589–597.

Pankratov Y, Lalo U, Verkhratsky A & North RA (2007). Quantal release of ATP in mouse cortex. *J Gen Physiol* **129**, 257–265.

Paton JF, De Paula PM, Spyer KM, Machado BH & Boscan P (2002). Sensory afferent selective role of P2 receptors in the nucleus tractus solitarii for mediating the cardiac component of the peripheral chemoreceptor reflex in rats. *J Physiol* **543**, 995–1005.

Paxinos G & Watson C (1986). *The Rat Brain in Stereotaxic Coordinates*. Academic Press Ltd, London.

Ralevic V, Thomas T, Burnstock G & Spyer KM (1999). Characterization of P2 receptors modulating neural activity in rat rostral ventrolateral medulla. *Neuroscience* **94**, 867–878.

Robson SC, Sevigny J & Zimmermann H (2006). The E-NTPDase family of ectonucleotidases: Structure function relationships and pathophysiological significance. *Purinergic Signal* **2**, 409–430.

Rong W, Gourine AV, Cockayne DA, Xiang Z, Ford AP, Spyer KM & Burnstock G (2003). Pivotal role of nucleotide $P2X_2$ receptor subunit of the ATP-gated ion channel mediating ventilatory responses to hypoxia. *J Neurosci* **23**, 11315–11321.

Sant'Ambrogio G (1982). Information arising from the tracheobronchial tree of mammals. *Physiol Rev* **62**, 531–569.

Sawada K, Echigo N, Juge N, Miyaji T, Otsuka M, Omote H, Yamamoto A & Moriyama Y (2008). Identification of a vesicular nucleotide transporter. *Proc Natl Acad Sci U S A* **105**, 5683–5686.

Thomas T & Spyer KM (2000). ATP as a mediator of mammalian central CO_2 chemoreception. *J Physiol* **523**, 441–447.

Vardhan A, Kachroo A & Sapru HN (1993). Excitatory amino acid receptors in commissural nucleus of the NTS mediate carotid chemoreceptor responses. *Am J Physiol Regul Integr Comp Physiol* **264**, R41–R50.

Wasserman AM, Sahibzada N, Hernandez YM & Gillis RA (2000). Specific subnuclei of the nucleus tractus solitarius play a role in determining the duration of inspiration in the rat. *Brain Res* **880**, 118–130.

Widdicombe J (2001). Airway receptors. *Respir Physiol* **125**, 3–15.

Yao ST, Barden JA, Finkelstein DI, Bennett MR & Lawrence AJ (2000). Comparative study on the distribution patterns of $P2X_1$-$P2X_6$ receptor immunoreactivity in the brainstem of the rat and the common marmoset (*Callithrix jacchus*): association with catecholamine cell groups. *J Comp Neurol* **427**, 485–507.

Yao ST, Barden JA & Lawrence AJ (2001). On the immunohistochemical distribution of ionotropic P2X receptors in the nucleus tractus solitarius of the rat. *Neuroscience* **108**, 673–685.

Yao ST, Gourine AV, Spyer KM, Barden JA & Lawrence AJ (2003). Localisation of $P2X_2$ receptor subunit immunoreactivity on nitric oxide synthase expressing neurones in the brain stem and hypothalamus of the rat: a fluorescence immunohistochemical study. *Neuroscience* **121**, 411–419.

Zhang W & Mifflin SW (1993). Excitatory amino acid receptors within NTS mediate arterial chemoreceptor reflexes in rats. *Am J Physiol Heart Circ Physiol* **265**, H770–H773.

Zhang W & Mifflin SW (1995). Excitatory amino-acid receptors contribute to carotid sinus and vagus nerve evoked excitation of neurons in the nucleus of the tractus solitarius. *J Auton Nerv Syst* **55**, 50–56.

Zhang M & Nurse CA (2004). CO_2/pH chemosensory signaling in co-cultures of rat carotid body receptors and petrosal neurons: role of ATP and ACh. *J Neurophysiol* **92**, 3433–3445.

Zhang M, Zhong H, Vollmer C & Nurse CA (2000). Co-release of ATP and ACh mediates hypoxic signalling at rat carotid body chemoreceptors. *J Physiol* **525**, 143–158.

Acknowledgements

We are grateful to the Biotechnology and Biological Sciences Research Council (K.M.S., A.V.G.) and The Wellcome Trust (A.V.G., N.D.) for financial support.